FEBS Letters 582 (2008) 3145–3151

Identification of nucleolar effects in JNK-deficient cells

Antoine Mialon[a,b,1], Jacob Thastrup[c,1], Tuula Kallunki[c], Leni Mannermaa[a], Jukka Westermarck[a,d], Tim H. Holmström[a,e,*]

[a] Center for Biotechnology, University of Turku and Åbo Akademi University, Artillerigatan 6, 20520 Turku, Finland
[b] Department of Medical Biochemistry, University of Turku, 20520 Turku, Finland
[c] Apoptosis Department, Institute of Cancer Biology, Danish Cancer Society, DK-2100 Copenhagen, Denmark
[d] Institute of Medical Technology, University of Tampere and Tampere University Hospital, 33520 Tampere, Finland
[e] VTT Medical Biotechnology, 20521 Turku, Finland

Received 29 May 2008; revised 2 August 2008; accepted 4 August 2008

Available online 12 August 2008

Edited by Angel Nebreda

Abstract **The c-Jun N-terminal kinase (JNK) signalling pathway has an established role in cellular stress signalling, cell survival and tumorigenesis. Here, we demonstrate that inhibition of JNK signalling results in partial delocalization of the RNA helicase DDX21 from the nucleolus to the nucleoplasm, increased nucleolar mobility of DDX21 and inhibition of rRNA processing. Furthermore, our results show that JNK signalling regulates DDX21 phosphorylation and protein expression. In conclusion, the results presented in this study reveal a previously unidentified cellular role for JNK signalling in the regulation of nucleolar functions. Based on these results, we propose that JNK-mediated effects on nucleolar homeostasis and rRNA processing should be considered when interpreting cellular phenotypes observed in JNK-deficient cell and animal models.**

Keywords: DDX21; JNK; Kinase; Nucleolus; Phosphorylation; RNA helicase

1. Introduction

All organisms need to respond to stress by different means in order to adapt to changes in their environment. Stress stimuli have been shown to activate the members of the mitogen-activated protein kinase family (MAPK), including the p38 MAPK, the ERK and the c-Jun protein kinases (JNK). The JNK pathway is activated upon different stress stimuli such as UV-B radiation, hyperosmotic shock and oxidative damage. Activated JNK is known to phosphorylate various target proteins such as c-Jun, ATF2 and Elk1 [1]. In addition to its functions in stress regulation, the JNK signalling pathway has an important role in the positive regulation of cell proliferation and survival and has therefore been implicated in tumorigenesis [2,3].

The nucleolus is a nuclear domain responsible for regulation of ribosome biogenesis, ribosomal (rRNA) processing, and compartmentalization of nuclear proteins [4]. The nucleolus comprise of a vast number of proteins with various functions and distinct nucleolar localization [5]. Recently, additional functions such as regulation of cell cycle, cellular stress response signalling and telomerase activity have been attributed to the nucleolus [4,6]. The nucleolus is known to respond rapidly to stress signals, and recent studies have characterized a plethora of proteins moving rapidly in or out from the nucleolus in response to cellular stress [7]. Furthermore, the rapid nucleolar translocation of the nucleolar proteins HDM2 and B23 upon DNA damage has been shown to be essential for a proper DNA damage response through stabilization of p53 protein levels [8,9].

Several recent studies have suggested a close connection between JNK signalling and nucleolar functions: stress-activated JNK inhibits ribosomal RNA (rRNA) synthesis through phosphorylation of the transcription factor TIF-IA [6], induces nucleoplasmic translocation of nucleolar RNA helicase DDX21 [10], and mediates stress-induced nucleolar shuttling of the nucleolar proteins B23 and p19Arf [11]. All these results clearly indicate that stress-induced JNK activation results in changes in both location and function of several nucleolar proteins.

In this study, we demonstrate that in addition to mediating cellular stress response, JNK signalling have an important role in the regulation of nucleolar homeostasis in non-stressed cells. We show that both genetic and chemical inhibition of JNK signalling results in partial nucleoplasmic translocation of DDX21. Our results indicate that the observed nucleolar translocation of DDX21 is possibly due to JNK-mediated phosphorylation. Moreover, chemical suppression of JNK signalling inhibits accumulation of the mature 18S and 28S rRNA subunits. Taken together, results presented here indicate a novel role for JNK signalling in maintaining nucleolar homeostasis and rRNA processing in non-stressed cells.

2. Materials and methods

2.1. Cell culture, cloning

HT1080 cells were obtained from ATCC. The c-Jun, JNK1 −/− and JNK2 −/− knockout mouse embryonal fibroblasts (MEFs) used for the study have been previously published [12,13]. The JNK null (JNK1,2 −/−) MEFs were established by crossing JNK2 −/− and JNK1 +/− mice. The embryos were isolated at E9. Heart, liver and head was removed and used for genotyping. The remaining embryonic tissue was homogenized with pipetting, plated on a six-well plate and

*Corresponding author. Address: Center for Biotechnology, University of Turku and Åbo Akademi University, Artillerigatan 6, 20520 Turku, Finland.
E-mail address: tholmstr@btk.fi (T.H. Holmström).

[1]These authors contributed equally to the work.

0014-5793/$34.00 © 2008 Published by Elsevier B.V. on behalf of the Federation of European Biochemical Societies.
doi:10.1016/j.febslet.2008.08.004

Table 1
Mutagenesis primers used to produce alanine EGFP-DDX21 mutants

Mutation	Sequences
S71A	5′-GAAGTTGACATGAAT**G**CTCCTAAATCCAAA-3′
S71Arev	5′-TTTGGATTTAGGAG**C**ATTCATGTCAACTTC-3′
S89A	5′-CCATCTCAAAATGACATT**G**CTCCTAAAACC-3′
S89Arev	5′-GGTTTTAGGAG**C**AATGTCATTTTGAGATGG-3′
S121A	5′-AAATGAGGAGCCT**G**CTGAGGAAGAAATAGA-3′
S121Arev	5′-TCTATTTCTTCCTCAG**C**AGGCTCCTCATTT-3′
S171A	5′-CTGCCAGTGAAGAA**GA**TAACAGTGAGATAG-3′
S171Arev	5′-CTATCTCACTGTTA**TC**TTCTTCACTGGCAGGGT-3′
L264A-L266A	5′-CCGTGCCCCTCAGGTA**GC**GGTT**GC**TGCACCTACAAGAGAGTTGG-3′
L264A-L266Arev	5′-CCAACTCTCTTGTAGGTGCA**GC**AACC**GC**TACCTGAGGGGCACGG-3′

Nucleotides in bold indicate the point mutations.

cultured in DMEM/F12 (Invitrogen) supplemented with 20% FCS (HyClone) and 10 μg/ml of Gentamycin (GIBCO). After 4 passages the cells were changed to DMEM (Invitrogen) supplemented with 10% FCS (HyClone), 4 μg/ml of non-essential amino acids, 10 μg/ml of Gentamycin (GIBCO). All cells were cultured at 37 °C in 5% CO_2 in Dulbecco's modified Eagle's medium (Invitrogen), supplemented with 10% heat-inactivated fetal calf serum (FCS; Invitrogen) and penicillin–streptomycin (100 IU/ml and 100 mg/ml, respectively). EGFP-DDX21 constructs were obtained from EGFP-DDX21 [14] following the QuikChange® II Site-Directed Mutagenesis Kit protocol (Stratagene). Mutagenesis primer sequences are listed in Table 1.

The HA-tagged c-Jun constructs, c-Jun WT, c-Jun$^{31–57}$ and c-Jun^{Ala} used in immunofluorescence are described elsewhere [15].

2.2. Immunofluorescence microscopy and photoswitch experiments

Immunostaining of cells grown on coverslips was performed by simultaneous fixation and permeabilization in 20 mM PIPES, pH 6.8, 4% formaldehyde, 0.2% Triton X-100, 10 mM EGTA, 1 mM $MgCl_2$, for 10 min at room temperature. Primary antibodies used were rabbit monoclonal c-Jun (Signal Transduction), mouse monoclonal HA (Santa Cruz Biotechnology) and human polyclonal DDX21 [16]. Primary antibodies were detected with Cy2- or Cy3-conjugated secondary antibodies (Jackson Immunoresearch). Wide-field fluorescence microscope images were collected using a Leica DMRE microscope equipped with a high resolution Hamamatsu Photonics ORCA C4742-95 CCD camera. Fluorescence intensities were determined using the Metamorph imaging software (Universal imaging). Relative nucleoplasm/nucleolus distribution of endogenous DDX21 protein was quantitated from a representative area of the nucleolus or nucleoplasm of 30–50 cells/group.

For FRAP studies cells were transfected with EGFP-DDX21 [14] and grown on glass plates (MatTek). Size and location of the photobleach or photoswithing area was adjusted with Zeiss LSM 510 version 3.2 software. Fluorescence intensities were measured using photomultiplier tubes connected to the microscope and analyzed using the Zeiss LSM 510 version 3.2 software, through FITC (Ex. 490BP10 nm, Em. 528BP19 nm). Digital images were superimposed and assembled in Adobe Photoshop software.

2.3. Quantification of protein levels

Samples of subconfluent HT1080, MEF wt or JNK1,2 −/− cells were processed and analysed by Western blotting using mouse monoclonal actin (Santa Cruz Biotechnology), rabbit monoclonal c-Jun (Signal Transduction), human polyclonal DDX21 [16] and JNK (Signal Transduction) antibodies. Quantifications have been done by MCID imaging analysis software.

2.4. Northern blotting

rRNA processing was studied using rRNA subunit-specific probes as described [17]. Shortly the total RNA was isolated using RNeasy (Qiagen). RNA was separated on a 1% agarose–formaldehyde gel and blotted on Hybond-N membranes (GE Healthcare). RNA was separated on a 1% agarose–formaldehyde gel and blotted on Hybond-N membranes. The autoradiogram was exposed and visualized using a PhosphorImager (Fuji). Quantifications have been done by MCID imaging analysis software.

2.5. Immunoprecipitation and ^{32}P in vivo labelling

For in vivo labelling experiments cells were preincubated in phosphate-free DME (GIBCO BRL) with 1% FCS for 60 min. The medium was then replaced by phosphate-free DME/10% FBS containing 0.5 mCi/ml ^{32}P-orthophosphate (GE Healthcare). After 3 h, the radioactive medium was removed and cells were lyzed in lysis buffer (1% Nonindent NP-40, 50 mM Tris, pH 7.4, 0,2 mM EDTA, 0,15 M NaCl, 0.5 mM dithiothreitol (DTT), 0.5 mM phenylmethylsulphonylfluoride (PMSF), 0.5% sodium deoxycholate, 1 mM Na_3VO_4, 1× complete protease inhibitor (Roche) for 30 min. The supernatant was incubated with the human polyclonal DDX21 [16] coupled to protein A Sepharose (Sigma). Immunoprecipitates were then washed three times in lysis buffer followed by addition of Laemmli sample buffer. The samples were resolved on 12.5% SDS–PAGE, and DDX21 phosphorylation was quantified using PhosphoImager (Fuji). Quantifications have been done by MCID imaging analysis software.

3. Results and discussion

3.1. JNK signalling promotes DDX21 nucleolar localization

Although our previous work demonstrated that c-Jun supports nucleolar localization of DDX21 [17], the role for JNK in the regulation of DDX21 nucleolar localization has not been demonstrated. As compared to wild-type mouse fibroblasts, clearly increased nucleoplasmic staining of DDX21 was observed in immortalized embryonal fibroblasts (MEFs) derived from JNK1,2 deficient mice (JNK1,2 −/−) (Fig. 1A). Quantitation of the ratio between nucleoplasmic and nucleolar DDX21 staining revealed that approximately twice as much DDX21 was localized to nucleoplasm in JNK1,2 −/− cells as compared to wild-type cells (Fig. 1B). This suggests that JNK activity supports nucleolar localization of DDX21. Interestingly, depletion of JNK1 or JNK2 alone did not produce any significant effects on DDX21 localization, suggesting that JNK isoforms have redundant functions in regulating DDX21 localization. Nucleoplasmic localization of DDX21 in JNK1,2 −/− cells was not due to any clonal effect, as a similar phenotype was observed in human HT1080 fibrosarcoma cells treated with the chemical JNK inhibitor SP600125 (Fig. 1C and D). No difference in DDX21 nucleolar localization was observed in HT1080 cells treated with the p38 kinase inhibitor SB302850 or the MEK1,2 inhibitor PD98059 (Fig. 1C and D). As no additive effect was observed when the JNK inhibitor SP600125 was added to the JNK1,2 −/− cells (Fig. 1E and F), this indicates that the observed effect of SP600125 on DDX21 nucleolar localization is specific for JNK signalling. These results demonstrate that JNK signalling supports DDX21 nucleolar localization in non-stressed conditions.

3.2. JNK signalling reduces nucleolar shuttling of DDX21

We and others have previously shown that DDX21 shuttles rapidly between the nucleolus and the nucleoplasm [7,18], and that c-Jun affects this shuttling [17]. Moreover, we have shown that nucleoplasmic re-localization of DDX21 correlates with an increase in its nucleolar mobility and decreased substrate binding capacity [17]. In order to obtain independent and quantitative evidence for the role of JNK signalling in the regulation of nucleolar localization of DDX21, we next studied the nucleolar–nucleoplasmic shuttling of EGFP-DDX21 in both non-treated and SP600125 treated HT1080 cells. To this end, selected nucleoli positive for EGFP-DDX21 were photoactivated and images were obtained at 30 s intervals and the inward nucleolar movement of DDX21 by fluorescence recovery

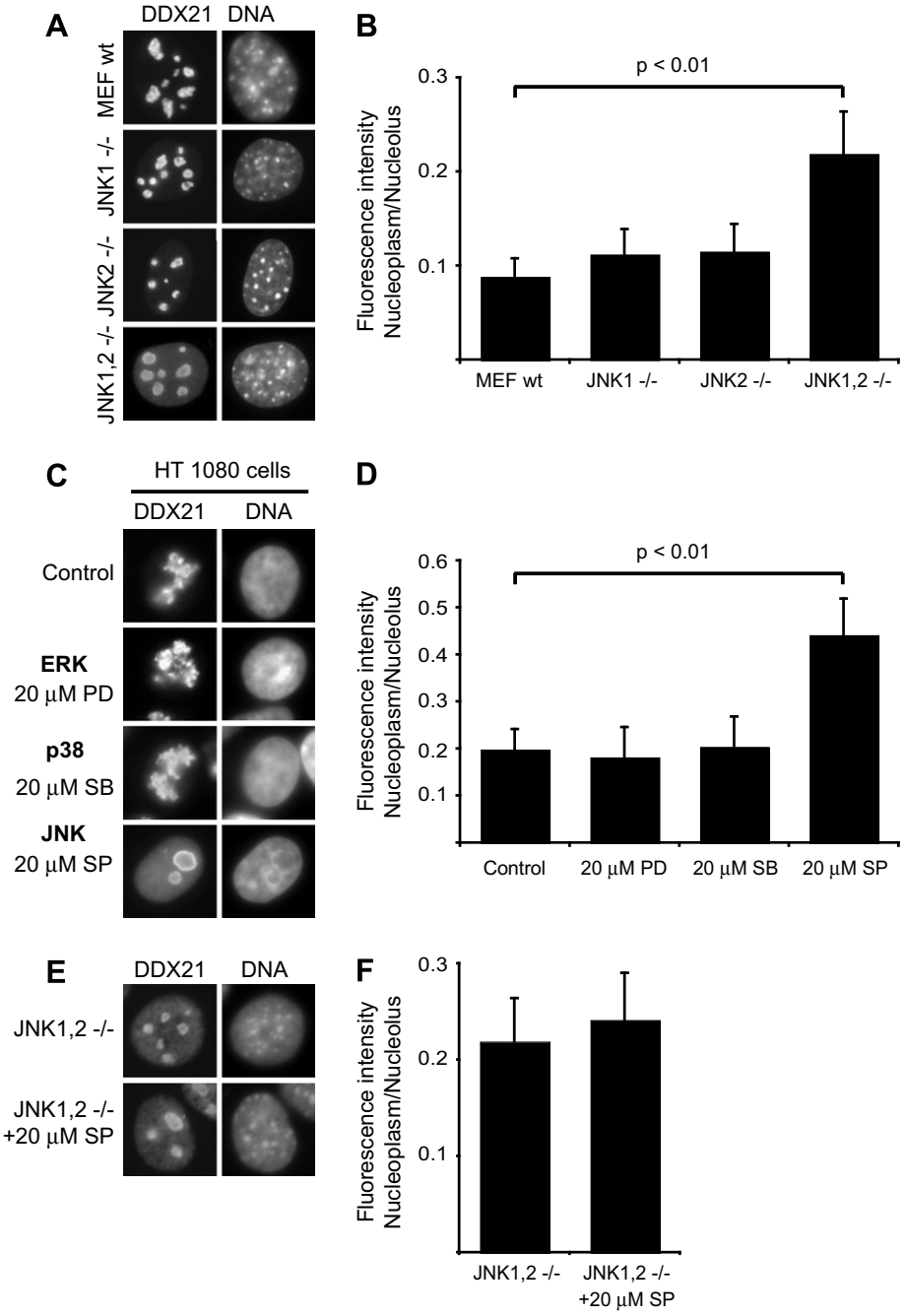

Fig. 1. JNK promotes nucleolar localization of DDX21. (A) Localization of endogenous DDX21 in wild-type, JNK1 −/−, JNK2 −/− and JNK1,2 −/− MEFs as examined by wide-field fluorescence microscopy. (B) A graph showing the ratio of DDX21 staining in nucleoplasm/nucleolus depicted as mean ± S.D. of 50 cells/group. (C) Localization of endogenous DDX21 in HT1080 cells 1 h after 20 μM PD98059, SB302850 and SP600125 treatment. (D) A graph showing the ratio of DDX21 staining in nucleoplasm/nucleolus depicted as mean ± S.D. of 50 cells/group. (E) Localization of endogenous DDX21 in non-treated or SP600125 treated JNK1,2 −/− MEFs as examined by wide-field fluorescence microscopy. (F) A graph showing the ratio of DDX21 staining in nucleoplasm/nucleolus depicted as mean ± S.D. of 50 cells/group. (A, C and E) Shown are images representing the dominant phenotype observed in the cell population. Each experiment was repeated two to three times with similar results.

after photobleaching (FRAP) of EGFP-DDX21 was measured. Fig. 2 shows a representative time series of photoactivated nucleoli in untreated and SP600125 treated cells (Fig. 2A). Quantitation of DDX21 half-time ($t_{1/2}$) for nucleolar recovery revealed a significantly shorter recovery time for EGFP-DDX21 in SP600125 treated HT1080 cells. The mean $t_{1/2}$ recovery time was 30 s in SP600125 cells compared to 150 s in untreated cells (Fig. 2B). These results, obtained by an independent method to study the effect of JNK signalling on DDX21 cellular localization, imply that JNK signalling stabilizes DDX21 nucleolar localization. Taken together with the data shown in Fig. 1, these results demonstrate a novel role for JNK signalling in regulating nucleolar shuttling of DDX21.

3.3. JNK signalling regulates DDX21 protein expression

As JNK signalling is known to regulate c-Jun protein expression, we examined the protein levels of c-Jun and DDX21 in JNK1,2 −/− cells. As shown in Fig. 3A the protein levels of c-Jun were decreased in JNK1,2 −/− cells and surprisingly also the protein levels of DDX21 (Fig. 3A). A clear decrease in DDX21 protein levels was also observed in HT1080 cells treated for 24 h with SP600125 (Fig. 3B). However, treatment with the JNK inhibitor SP600125 for 1 h did not have a clear effect on the protein levels of c-Jun, DDX21 and JNK in wild-type MEFs (Fig. 3A). Therefore, the effects of SP600125 on DDX21 localization (Fig. 1), shuttling (Fig. 2) and phosphorylation (Fig. 4A) are likely not due to decreased DDX21 protein levels. These results implicate that JNK signalling not only promotes nucleolar localization of DDX21 but also supports DDX21 expression.

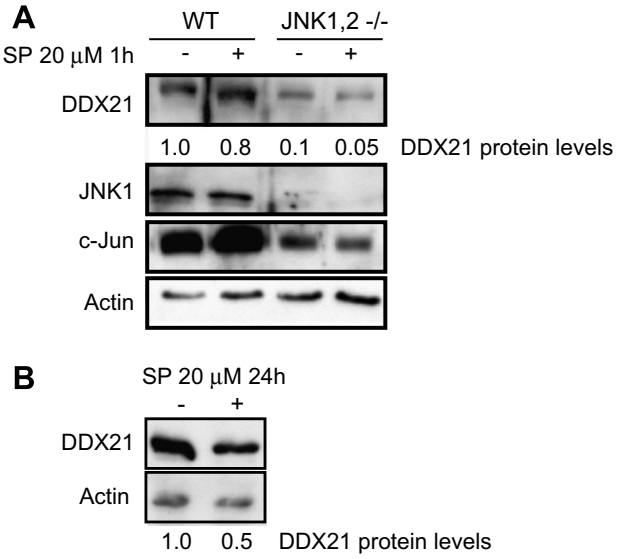

Fig. 3. c-Jun and DDX21 levels are reduced in JNK1,2 −/− cells. (A) The protein levels of actin, c-Jun, DDX21 and JNK1 in MEF WT and JNK1,2 −/− whole cell extract was examined by Western blot analysis of the respective proteins. Quantification of the DDX21 protein expression levels is also shown. Quantitation has been done by MCID imaging analysis software and correlated to actin expression from the same sample. (B) The protein levels of actin, c-Jun, DDX21 and phospho-c-Jun in untreated and SP600125 treated (20 μM, 24 h) HT1080 cells whole cell extract was examined by Western blot analysis of the respective proteins. (A and B) Quantitation of the DDX21 protein expression levels correlated to actin expression from the same sample.

3.4. JNK regulates DDX21 phosphorylation

One putative mechanism by which JNK signalling could regulate DDX21 nucleolar localization is by protein phosphorylation. To study this possibility, we compared DDX21 ^{32}P labelling between control and SP600125 treated HT1080 cells. In addition, DDX21 phosphorylation was compared between JNK1,2 −/− and c-Jun −/− MEFs, both displaying partial nucleoplasmic localization of DDX21 (Fig. 1). As shown in

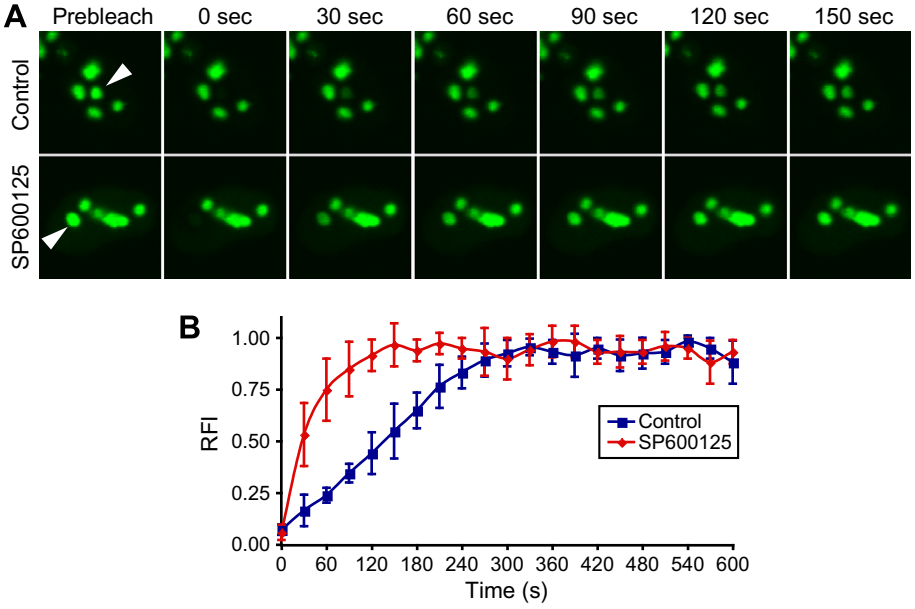

Fig. 2. JNK inhibits DDX21 nucleolar mobility. (A) Exogenously expressed EGFP-DDX21 proteins in untreated or SP600125 treated (20 μM, 1 h) HT1080 cells was subjected to photobleach by a 488 nm laserline in indicated nucleoli (white arrowheads). FITC (515 nm) shows recovery of the photobleached EGFP-DDX21 proteins. (B) Quantitation of the nucleolar recovery rate of EGFP-DDX21 in untreated or SP600125 treated cells as measured by relative fluorescence intensity passing through the 515 nm filter.

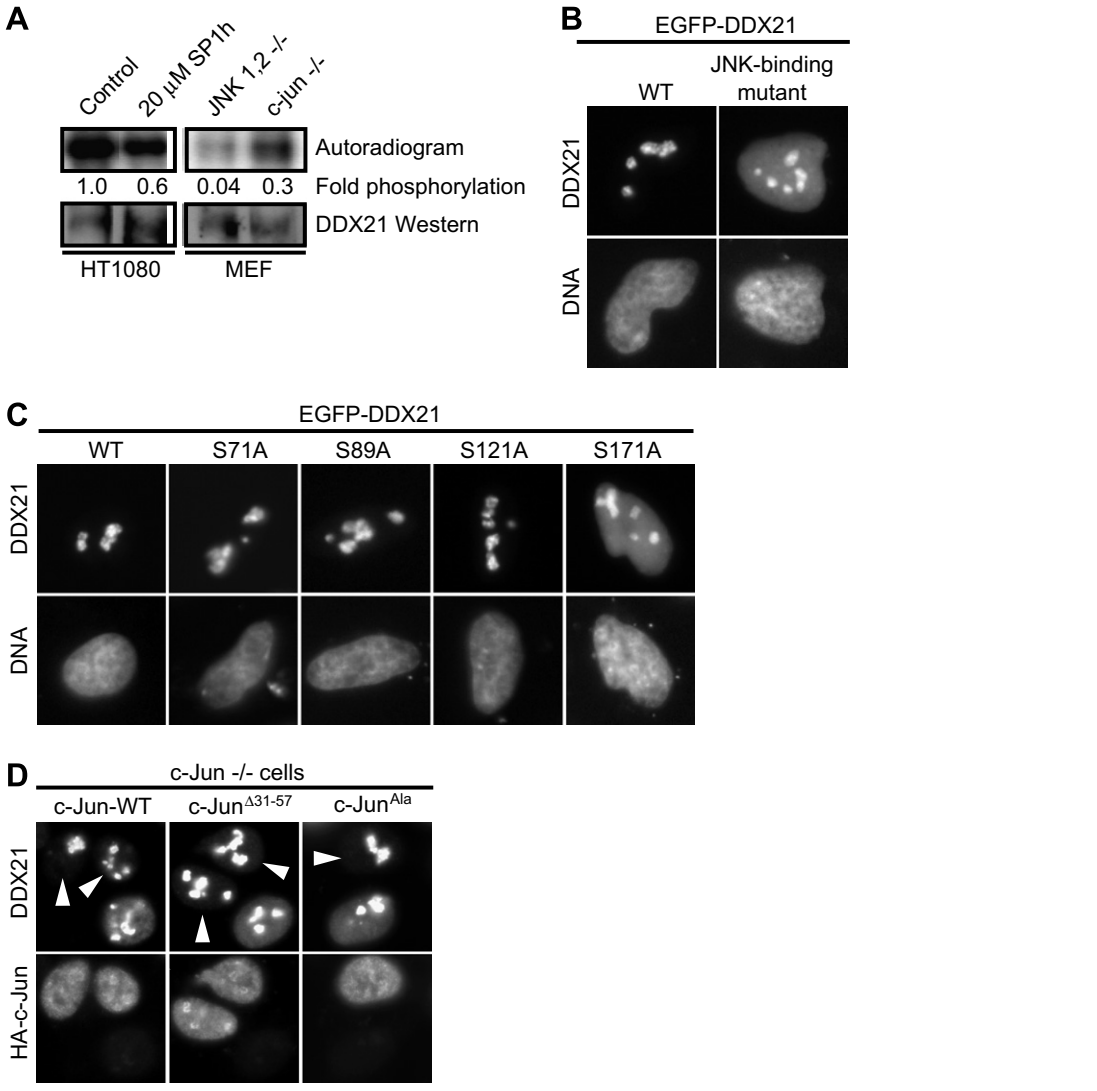

Fig. 4. JNK affects DDX21 phosphorylation status. (A) DDX21 phosphorylation status was examined by ^{32}P in vivo labelling and DDX21 immunoprecipitation in non-treated and SP600125 (20 μM, 1 h) treated HT1080 cells as well as in c-Jun −/− and JNK1,2 −/− MEF cells. The upper panel shows an autoradiogram of DDX21 and the lower panel a DDX21 Western blot. Quantitation of DDX21 phosphorylation levels correlated to immunoprecipitated DDX21 protein levels from the same sample. (B) Localization of EGFP-DDX21 wt, a putative EGFP-DDX21 JNK binding mutant as examined by wide-field fluorescence microscopy. (C) Wide-field images of EGFP-DDX21 wt, EGFP-DDX21 S71A, EGFP-DDX21 S89A, EGFP-DDX21 S121A, EGFP-DDX21 S171A. (D) Wild-type (c-Jun-WT), JNK-binding (c-Jun$^{\Delta 31-57}$) and phosphorylation (c-Jun^{Ala}) deficient HA-tagged c-Jun rescues nucleolar localization of DDX21 in Jun −/− MEFs. Transfected HA-positive cells are indicated by white arrowheads. (A–D) Shown are images representing the dominant phenotype observed in the cell population. Each experiment was repeated two to three times with similar results.

Fig. 4A, DDX21 phosphorylation was diminished in SP600125 treated (1 h) cells. Moreover, DDX21 phosphorylation was clearly decreased in JNK1,2 −/− cells as compared to c-Jun −/− cells (Fig. 4A). These results demonstrate that JNK activity increases DDX21 phosphorylation and suggests that even though comparable DDX21 re-localization is seen in both JNK1,2 −/− and c-Jun −/− cells, the mechanism by which JNK and c-Jun regulate DDX21 localization might be different. In order to study more closely how JNK affects DDX21 localization we mutated two leucines to alanine of the potential JNK-binding site ([1]; LVL; L262A, L264A) on DDX21, and studied the nucleolar localization of DDX21. Interestingly, DDX21 harbouring a mutation in the putative JNK binding site was clearly more localized to the nucleoplasm than the wild-type DDX21 (Fig. 4B). Several reports have independently identified the serines; 71, 89, 121, 171 as phosphorylated on DDX21 [19,20]. Of these sites serine S171 has a proline in +1 position, making it a potential phosphorylation site for JNK [1]. To study if any of the serines are important for DDX21 nucleolar localization we made serine to alanine point mutations on these sites and studied the nucleolar localization of DDX21 (Fig. 4C). As evident from Fig. 4C, a mutation of serine 171 to alanine (S171A) clearly resulted in a nucleoplasmic localization of DDX21, whereas mutation of serines 71 (S71A), 89 (S89A), or 121 (S121A), did not affect DDX21 nucleolar localization. These results together suggest that JNK signalling regulates DDX21 nucleolar localization through a phosphorylation-dependent mechanism.

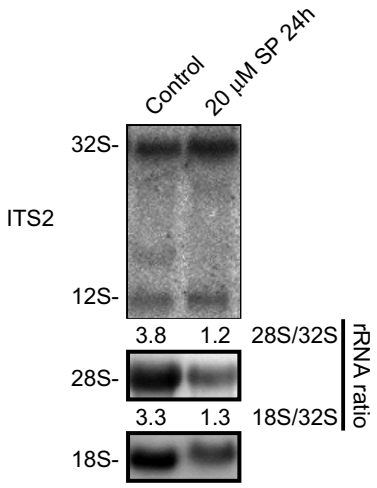

Fig. 5. Chemical suppression of JNK activity inhibits 28S and 18S rRNA accumulation. 32S, 28S, 18S and 12S rRNA subunit abundance was examined by Northern blot analysis in non-treated and SP600125 (20 μM, 24 h) treated HT1080 cells. Fold differences in rRNA accumulation are indicated in relation to 32S rRNA.

3.5. c-Jun and JNK regulate DDX21 nucleolar localization through different mechanisms

We recently demonstrated that c-Jun depletion results in similar nucleoplasmic relocalization of DDX21 as is observed here with JNK inhibition [17]. On the other hand our results above show different levels of DDX21 phosphorylation in c-Jun or JNK depleted cells (Fig. 4A). We therefore next studied whether inhibition of JNK regulates DDX21 nucleolar localization through phosphorylation of c-Jun. To this end, we studied if a transiently transfected c-Jun WT, JNK-deficient binding mutant of c-Jun (c-Jun$^{\Delta 31-57}$) and a c-Jun mutant where the known JNK phosphorylation sites on c-Jun, Serine 63 and 73 and Threonine 91 and 93, are mutated to Alanine (c-Jun^{Ala}) [15], are able to rescue the nucleoplasmic localization of DDX21 in c-Jun −/− cells. As shown in Fig. 4D, c-Jun WT, c-Jun$^{\Delta 31-57}$ and c-Jun^{Ala} all rescued DDX21 nucleolar localization in c-Jun −/− cells indicating that c-Jun-mediated regulation of DDX21 localization is independent of its JNK-mediated phosphorylation. These results indicate that JNK-c-Jun signalling pathway supports DDX21 nucleolar localization, but that both JNK and c-Jun exert their effects on DDX21 at least partly by independent mechanisms.

3.6. JNK signalling reduces rRNA processing

It is well established that rRNA processing occurs in the nucleolus and that the RNA helicase DDX21 plays a role in this process [4,5,16]. We recently reported that c-Jun regulates DDX21's nucleolar localization and rRNA processing [17]. As, we show in this study that JNK signalling regulates DDX21's nucleolar localization and protein levels we next wanted to study whether JNK signalling also affect rRNA processing. In order to study the effect of JNK signalling on rRNA processing the steady state abundance of 32S, 28S, 18S and 12S rRNA in non-treated and SP600125 treated (24 h) HT1080 cells was quantified by Northern blot analysis. Fig. 5 clearly shows that suppression of JNK signalling by SP600125 results in inhibition of 28S and 18S rRNA accumulation. Therefore, JNK signalling not only regulates the nucleolar localization of DDX21 but leads to inhibition of rRNA processing. Taken together, this work demonstrates that JNK signalling regulates DDX21 localization, protein levels and rRNA processing in non-stressed cells. As both stress-elicited JNK activation [10], and JNK inhibition (Fig. 1) affects nucleolar localization of DDX21, it indicates that there exists a delicate balance in the regulation of DDX21 nucleolar localization in both resting and stressed cells.

In conclusion our results clearly indicate that phenotypes previously observed in JNK depleted cells [1–3] might not only be mediated by the already identified JNK substrates, but could be at least partly due to nucleolar JNK effects reported in this study.

Acknowledgements: We thank D. Gillespie for the c-Jun −/− MEF. This work was supported by funding from the Academy of Finland (Projects 878179 and 8212695), Sigrid Juselius Foundation and Finnish Cancer Association. T.H.H. is supported by a Human Frontier Science Program Organization Long-Term Fellowship, Stiftelsen för Åbo Akademis Forskningsinstitut and The Foundation for the Finnish Cancer Institute. J.T. and T.K. are supported by the Danish Cancer Society.

References

[1] Davis, R.J. (2000) Signal transduction by the JNK group of MAP kinases. Cell 103, 239–252.
[2] Eferl, R. and Wagner, E.F. (2003) AP-1: a double-edged sword in tumorigenesis. Nat. Rev. Cancer 3, 859–868.
[3] Manning, A.M. and Davis, R.J. (2003) Targeting JNK for therapeutic benefit: from junk to gold? Nat. Rev. Drug Discov. 2, 554–565.
[4] Lam, Y.W., Trinkle-Mulcahy, L. and Lamond, A.I. (2005) The nucleolus. J. Cell Sci. 118, 1335–1337.
[5] Boisvert, F.M., van Koningsbruggen, S., Navascues, J. and Lamond, A.I. (2007) The multifunctional nucleolus. Nat. Rev. Mol. Cell. Biol. 8, 574–585.
[6] Mayer, C., Bierhoff, H. and Grummt, I. (2005) The nucleolus as a stress sensor: JNK2 inactivates the transcription factor TIF-IA and down-regulates rRNA synthesis. Genes Dev. 19, 933–941.
[7] Andersen, J.S., Lam, Y.W., Leung, A.K., Ong, S.E., Lyon, C.E., Lamond, A.I. and Mann, M. (2005) Nucleolar proteome dynamics. Nature 433, 77–83.
[8] Rubbi, C.P. and Milner, J. (2003) Disruption of the nucleolus mediates stabilization of p53 in response to DNA damage and other stresses. EMBO J. 22, 6068–6077.
[9] Kurki, S., Peltonen, K. and Laiho, M. (2004) Nucleophosmin, HDM2 and p53: players in UV damage incited nucleolar stress response. Cell Cycle 3, 976–979.
[10] Westermarck, J. et al. (2002) The DEXD/H-box RNA helicase RHII/Gu is a co-factor for c-Jun-activated transcription. EMBO J. 21, 451–460.
[11] Yogev, O., Saadon, K., Anzi, S., Inoue, K. and Shaulian, E. (2008) DNA damage-dependent translocation of B23 and p19 ARF is regulated by the Jun N-terminal kinase pathway. Cancer Res. 68, 1398–1406.
[12] Nielsen, C., Thastrup, J., Bottzauw, T., Jaattela, M. and Kallunki, T. (2007) c-Jun NH2-terminal kinase 2 is required for Ras transformation independently of activator protein 1. Cancer Res. 67, 178–185.
[13] MacLaren, A., Black, E.J., Clark, W. and Gillespie, D.A. (2004) c-Jun-deficient cells undergo premature senescence as a result of spontaneous DNA damage accumulation. Mol. Cell. Biol. 24, 9006–9018.
[14] Valdez, B.C., Perlaky, L., Cai, Z.J., Henning, D. and Busch, H. (1998) Green fluorescent protein tag for studies of drug-induced translocation of nucleolar protein RH-II/Gu. Biotechniques 24, 1032–1036.
[15] Treier, M., Bohmann, D. and Mlodzik, M. (1995) JUN cooperates with the ETS domain protein pointed to induce photoreceptor R7 fate in the Drosophila eye. Cell 83, 753–760.

[16] Valdez, B.C., Henning, D., Busch, R.K., Woods, K., Flores-Rozas, H., Hurwitz, J., Perlaky, L. and Busch, H. (1996) A nucleolar RNA helicase recognized by autoimmune antibodies from a patient with watermelon stomach disease. Nucleic Acids Res. 24, 1220–1224.
[17] Holmstrom, T.H. et al. (2008) c-Jun supports ribosomal RNA processing and nucleolar localization of RNA helicase DDX21. J. Biol. Chem. 283, 7046–7053.
[18] Phair, R.D. and Misteli, T. (2000) High mobility of proteins in the mammalian cell nucleus. Nature 404, 604–609.
[19] Beausoleil, S.A. et al. (2004) Large-scale characterization of HeLa cell nuclear phosphoproteins. Proc. Natl. Acad. Sci. USA 101, 12130–12135.
[20] Olsen, J.V., Blagoev, B., Gnad, F., Macek, B., Kumar, C., Mortensen, P. and Mann, M. (2006) Global, in vivo, and site-specific phosphorylation dynamics in signaling networks. Cell 127, 635–648.